



Scientific Research

## Evaluation of physicochemical properties of extracted cellulose from the walnut shell using non-thermal plasma pretreatment

Sadat Anari, E. <sup>1</sup>, Soltanizadeh, N. <sup>2\*</sup>

1. M.Sc., Department of Food Science and Technology, College of Agriculture, Isfahan University of Technology, Isfahan, Iran.
2. Associate Professor, Department of Food Science and Technology, College of Agriculture, Isfahan University of Technology, Isfahan, Iran.

### ABSTRACT

The present study aims to extract cellulose fibers from the walnut shell using dielectric barrier discharge (DBD) plasma pretreatment and to evaluate its properties. For this purpose, powdered walnut shells were exposed to 18 and 20 kV DBD plasma for 10 min in three stages. First, before sodium hydroxide alkaline treatment, next, before sodium chlorite bleaching treatment, and then, before both alkaline and bleaching treatments. The extraction efficiency, FTIR, XRD, thermal properties, FESEM and diameters of the cellulose fiber were evaluated. Based on the results, the extraction efficiency was significantly affected by applied voltage ( $p < 0.05$ ) and due to plasma destruction of glycosidic, the efficiency was reduced. The removal of peaks related to impurities from the walnut shell and the purity of all extracted cellulose was confirmed with FTIR. The results showed that applying DBD plasma during cellulose extraction did not affect its crystal structure, but the reduction of crystallization index was observed. Furthermore, the effect of plasma on the thermal-gravimetry of the samples was observed at temperatures below 100 °C, and after the onset temperature of degradation, the behavior of the treated and untreated fibers until the final thermal decomposition was not significantly different. The microstructure of plasma-treated samples showed an increase in cellulose fiber's roughness and swelling, followed by the transformation of microfibrils to nanofibrils with a diameter of 80 nm at the higher voltage. In general, the results showed that applying 20 kV DBD plasma in both stages before the alkaline and delignification process is a more suitable treatment for extracting cellulose and producing cellulose nanofibers.

### ARTICLE INFO

#### Article History:

Received 2022/ 06/ 29  
Accepted 2023/ 03/ 15

#### Keywords:

DBD plasma,  
Cellulose,  
Walnut shell,  
Structural properties.

DOI: 10.22034/FSCT.20.134.17  
DOR: 20.1001.1.20088787.1402.20.134.2.6

\*Corresponding Author E-Mail:  
soltanizadeh@iut.ac.ir

## 1. Introduction

Cellulose is the most abundant natural biopolymer in the structure of lignocellulosic fibers. Chemical structure of cellulose in 1920 by Hermann Stöding<sup>1</sup> It was found. This linear carbohydrate is composed of repeating D-glucopyranose units with (4→1) β glycosidic connections. In each monomer unit in the cellulose chain, three carbon atoms (C<sub>2</sub>-C<sub>3</sub>-C<sub>6</sub>) are attached to hydroxyl groups. The ability of these hydroxyl groups to establish hydrogen bonds plays an important role in controlling the physicochemical properties and microstructure formation of cellulose. The amount and properties of the extracted cellulose depend on the extraction process, origin and lifespan of the natural source [1]. So far, cellulose has been extracted from various lignocellulosic wastes such as soybean husk [2], peanut shell [3], rice straw [4], sugarcane bagasse [5], sweet corn [6] and other agricultural residues [7]. Different methods. To extract cellulose from biomass, these methods include chemical treatments including the use of acid and alkali [8], physical treatments including steam explosion, ultrasound [9] and extrusion [2], biological treatment including enzymatic hydrolysis [10] and combined processes. It includes acid-enzyme treatment [6] and radiation-enzyme treatment [5]. Since the structure of lignocellulosic materials is complex and the conventional methods used are usually polluting and consume a lot of energy, therefore it is necessary to replace these methods with environmentally friendly methods. One of the methods that is considered as an environmentally friendly method today It is a non-thermal plasma method.

Plasma is known as the fourth state of matter and is electrically almost neutral and consists of ions, free electrons, ultraviolet photons, radicals, atoms and molecules at the ground or excited level [12,11]. When the energy is transferred to neutral

natural gases, some of the gas components turn into charged particles to form plasma. This energy includes electricity, heat, light (ultraviolet light), radioactive rays (gamma rays) and electromagnetic radiation. Plasma produced by electric and electromagnetic fields is usually called electric discharge [13,11]. The origin of electric discharge production depends on the structure of the equipment and includes various types. Dielectric barrier discharge plasma is one of the non-thermal atmospheric pressure plasma production equipment, which includes two metal electrodes made of aluminum, brass or copper, which are flat and parallel, and at least one of these electrodes is protected by a dielectric layer such as ceramic, quartz, Bespar or covered with glass. The dielectric layer as a stabilizer prevents any displacement of the arc. This has caused dielectric barrier discharge to be one of the safe discharge methods [14, 12].

Plasma has been used so far to modify cellulose or decompose compounds with cellulose. Cora et al. (2014) investigated the effect of oxygen atmospheric pressure plasma on the efficiency of lignin degradation in sugarcane bagasse. The results showed that after plasma treatment, the efficiency of lignin removal improved by 5% and hemicellulose was removed to a small extent. In the samples with dimensions less than 1 mm, a small amount of destruction in the cellulose structure was also observed [15]. In another study, the effect of atmospheric pressure plasma treatment on the enzymatic hydrolysis of wheat straw lignocellulosic particles to constituent monosaccharides was investigated. The results showed that the hydrolysis of carbohydrates into glucose and xylose increased significantly in pretreated wheat straw. Also, the amount of lignin decreased in samples treated with plasma [16]. However, this method has not been used to extract cellulose. Therefore, in this research, walnut shell was selected as lignocellulosic raw

---

<sup>1</sup>. Hermann Staudinger

material, so that by using the special characteristics of cold plasma, this method can be used as a pre-treatment for cellulose extraction, and at the same time, the effect of this treatment on the characteristics of extracted cellulose is investigated.

## 2- Materials and methods

### 2-1- Materials

Walnut skin was collected from the gardens of Kurdistan. Sodium hydroxide (Dr. Majalli, Iran), sodium chlorite (Samchun, Korea) and diethyl ether (Pars, Iran) were purchased. Other chemicals used in this study were obtained from Merck, Germany.

### 2-2-extraction of cellulose fibers

First, walnut bark was crushed using a sk1 hammer mill (Retsch, Germany) and sieved using a 120 mesh sieve to obtain uniform powder particles. Then, the fat powder obtained by the Soxhlet method was removed with the help of diethyl ether solvent. To obtain the control sample, the sample was degreased with a fiber to solution ratio of 50:1 with 1 M sodium hydroxide solution in order to remove hemicellulose in a water bath with stirring at 85 Celsius was heated for 4 hours. Then the solution was filtered using a filter paper and washed with distilled water until the water leaving the filter became colorless and neutral. This process was repeated 5 times. The materials obtained from this step were mixed with 1.7% (weight/volume) sodium chlorite solution, whose pH reached 4 with acetic acid, in a 75 degree Celsius stirring water bath for 4 hours to remove lignin and decolorize. Then the solution was filtered using filter paper and washing with distilled water continued until the output water became colorless and neutral. The fibers obtained from this step were placed in a

moving air oven at a temperature of 80 degrees for drying [17].

In order to apply cold plasma pretreatment, an atmospheric pressure dielectric barrier plasma device (Yaran Fan Poya Exploration, Iran) was used. 2 grams of the sample was placed in a glass petri dish. The upper electrode was brought down until touching the petri lid, in which case the distance between the two electrodes was 1 cm. Plasma pretreatment was used in three stages and at two voltages of 18 and 20 kV for 10 minutes according to Table 1 during the cellulose extraction process. The efficiency of cellulose extraction was calculated using the gravimetric method and according to equation (1) [17].

Equation (1)

$$100 \times \text{Initial weight of material} / \text{weight of extracted cellulose} = (\%) \text{ yield}$$

In order to identify functional groups and investigate changes in the chemical structure of the samples, Fourier transform infrared spectrometer (FTIR)<sup>2</sup>Tensor 27 model (Brucker company, USA) in the wavelength range of  $\text{cm}^{-1}$  400-4000 was used [17].

crystal clear<sup>3</sup> Samples using X-ray diffractometer<sup>4</sup>(Philips, Netherlands) was determined. This means crystallinity index<sup>5</sup>Using Segal's experimental method<sup>6</sup> et al. (1959) was determined (Equation 2).

Equation (2)  $100 \times \frac{I_{\max} - I_{\min}}{I_{\max}} \times 100$  CrI% =  $I_{\max}$  .

$$\frac{I_{\max} - I_{\min}}{I_{\max}}$$

The CrI% index indicates the total amount of cellulose crystallinity,  $I_{\min}$ The minimum intensity measured in the angle range of  $2\theta=16^{\circ}$ - $22^{\circ}$  and  $I_{\max}$ The maximum intensity measured in the angle range of  $2\theta=22^{\circ}$ - $24^{\circ}$ . Also, to determine the dimensions of crystals from equation 3 known as Scherrer's equation<sup>7</sup> was used

<sup>2</sup>. Fourier transform infrared spectroscopy

<sup>3</sup>. Crystallinity

<sup>4</sup>. X-ray diffractometer

<sup>5</sup>. Crystalline index

<sup>6</sup>. Segal

<sup>7</sup>. Scherrer

$$\text{Equation (3)} \quad \theta \cos \beta / \lambda K L = \frac{K \lambda}{\beta \cos \Theta}$$

In this equation,  $L$  is the average crystal size in nanometers,  $K$  is Scherer's constant and is equal to 0.94,  $\lambda$  is the wavelength of the radiation and is equal to 0.154 nm,  $\beta$  is the width in half of the peak height.<sup>8</sup> In terms of radians and  $\theta$ , the diffraction angle of the leaf<sup>9</sup> is [5].

In order to check the thermal stability of the samples, from the thermal gravimeter (TGA)<sup>10</sup>(NETZSCH, Germany) was used under nitrogen gas atmosphere from room temperature to 600 degrees Celsius with a temperature change rate of 10 degrees Celsius per minute and the weight loss of the samples was plotted as a function of temperature [18].

In order to observe the microstructure of the samples and evaluate the size of the particles from the field emission scanning electron microscope (FE-SEM).<sup>11</sup>(FEI, America) was used [19]. The images were examined at a magnification of 10000. Also, the average fiber diameter was obtained by measuring the diameter of 12 different fibers and using ImageJ software.

### 2-3- Statistical analysis

The statistical analysis of the obtained results was done using the minimum significant difference test in the form of a completely randomized design. All the tests were performed in at least three repetitions and the results were evaluated using SAS software at a confidence level of 95%.

## 3- Results and discussion

### 3-1- Cellulose extraction efficiency

The results of plasma effect on cellulose extraction efficiency are shown in Table 2. As can be seen, the cellulose extraction efficiency was affected by the applied voltage ( $p < 0.05$ ). The maximum efficiency was observed in the control sample and with the application of plasma

treatment, the efficiency decreased so that the minimum efficiency with a difference of 4% from the control sample was observed in the sample treated with plasma at a voltage of 20 kV before the alkaline treatment and dye removal processes. This can be due to the destruction of the cellulosic fiber surface (Figure 4).

Also, according to the results of the Fourier transform infrared spectrometer, the decrease in the yield intensity in this sample can be due to the decomposition of the cellulose fibers, which happened both in the glucose rings and in the glycosidic bonds. It seems that due to the chemical and mechanical effects of plasma, the cellulose fibers are broken into their monomeric units in some places and removed during various chemical treatments and washing steps. These results confirmed the results of the study of Shaghaleh et al. (2019), who reported the weakening of the connection strength in the structure of lignocellulosic fibers of wheat stem and the increase in the solubility of carbohydrates due to severe plasma treatments [16].

Also, in the study of Souza et al. (2014), the effect of atmospheric pressure cold plasma pretreatment on the lignocellulosic compounds of sugarcane bagasse was investigated. Their results showed that in fibers with dimensions less than 1 mm, due to the greater effect of plasma and ozone treatment on the fibers, the cellulose content of the fibers decreased [15]. In general, the results showed that the use of plasma treatment before the alkaline treatment process had the least effect on the yield, which could be due to the presence of larger amounts of impurities and spending plasma energy in breaking the bonds of impurities with cellulose.

<sup>8</sup> . Full width half maximum

<sup>9</sup> . Bragg reflection angle

<sup>10</sup> . Thermogravimetric analysis

<sup>11</sup> . Field emission scanning electron microscope

**Table 1** Pre-treatment conditions applied to extract cellulose from walnut shell

| Applying DBD cold plasma pretreatment   |            |              | Sample  |   |
|---|------------|--------------|---------|---|
| Plasma treatment                        | hour (min) | Voltage (kV) |         |   |
| -                                       | -          | -            | Control | 1 |
| Before alkaline treatment               | 10         | 18           | A18     | 2 |
| Before bleaching treatment              | 10         | 18           | B18     | 3 |
| Before alkaline and bleaching treatment | 10         | 18           | AB18    | 4 |
| Before alkaline treatment               | 10         | 20           | A20     | 5 |
| Before bleaching treatment              | 10         | 20           | B20     | 6 |
| Before alkaline and bleaching treatment | 10         | 20           | AB20    | 7 |

**Table 2** Cellulose extraction efficiency

| Efficiency (%)            | Sample  |
|---------------------------|---------|
| 0.31 <sup>A</sup> ± 08.26 | Control |
| 0.31 <sup>A</sup> ± 25.91 | A18     |
| 0.42 <sup>C</sup> ± 23.58 | B18     |
| 0.51 <sup>D</sup> ± 22.58 | AB18    |
| 0.31 <sup>B</sup> ± 24.58 | A20     |
| 0.42 <sup>C</sup> ± 23.41 | B20     |
| 0.31 <sup>D</sup> ± 22.08 | AB20    |

Various letters in each column show significant differences among mean values ( $p < 0.05$ ).

A18: Cellulose extracted by 18 kV plasma pretreatment before alkaline treatment, B18: Cellulose extracted by 18 kV plasma pretreatment before bleaching treatment, AB18: Cellulose extracted by 18 kV plasma pretreatment before alkaline and bleaching treatment, A20: Cellulose extracted by 20 kV plasma pretreatment before alkaline treatment, B20: Cellulose extracted by 20 kV plasma pretreatment before bleaching treatment, AB20: Cellulose extracted by 20 kV plasma pretreatment before alkaline and bleaching treatment

### 2-3- Fourier transform infrared spectrometer

The curves obtained from the infrared spectrometer of the samples are shown in Figure

1. pass band in the range of cm wave number<sup>-1</sup>3300-3500 is related to the stretching vibration of free OH groups and intra- and intermolecular hydrogen bonds [17].

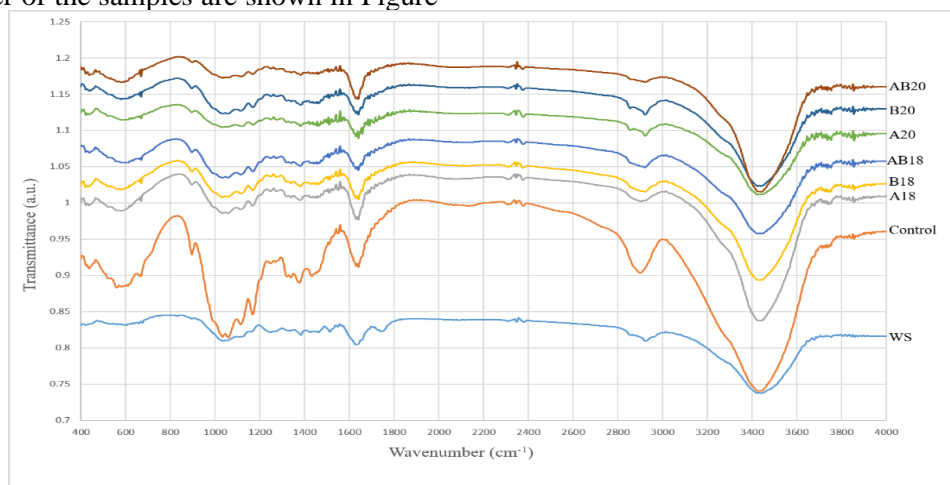


**Fig 1** FTIR spectra of Control, A18: Cellulose extracted by 18 kV plasma pretreatment before alkaline treatment, B18: Cellulose extracted by 18 kV plasma pretreatment before bleaching treatment, AB18: Cellulose extracted by 18 kV plasma pretreatment before alkaline and bleaching treatment, A20: Cellulose extracted by 20 kV plasma pretreatment before alkaline treatment, B20: Cellulose extracted by 20 kV plasma pretreatment before bleaching treatment, AB20: Cellulose extracted by 20 kV plasma pretreatment before alkaline and bleaching treatment, and WS: walnut shell.

Band available in cm wave number<sup>-1</sup>2850-2900 indicates C-H symmetric stretching vibration. The presence of water by the band placed in the

range of cm<sup>-1</sup>1636 is identified, which is related to the bending vibration of O-H groups of cellulose [20]. Passing band in the region of cm<sup>-1</sup>

$1429$  in the spectroscopic curve related to CH bending vibration<sub>2</sub>Symmetrical at carbon 6 ( $C_6$ ) that this band is known as crystal band. Also, the C-H bending vibrations in the plane cause a band in the range of  $cm^{-1}$ It will be  $1375$  [5]. Band observed in  $cm$  region<sup>-1</sup> $1161$  is related to the symmetric stretching vibration of C-O and C-C functional groups and the band in the region of  $cm^{-1}$   $1110$  is caused by C-O-C symmetric stretching [21]. Absorption bands in  $cm^{-1}$  $1030$ - $1060$  and  $cm^{-1}$   $896$  also indicate the stretching vibration of C-O in the pyranose ring and the bending vibration of  $\beta$ -glycosidic bonds in the structure of the cellulose molecule [22]. In the curve of untreated walnut skin, there is a band in  $cm^{-1}$  $1739$  is related to the stretching vibration of C=O carbonyl groups and indicates aldehyde, ketone or carboxylic acids in hemicellulose. The band seen in the region of  $cm^{-1}$  $1245$  indicates the stretching vibration of the C-O bond in the benzene ring of lignin and xylan hemicellulose molecules [23,5].  $cm$  band<sup>-1</sup> $1512$  is also related to the stretching vibration of the C=C aromatic ring in lignin [24]. Removing these three bands in the curveThe data related to the control sample and the samples treated with plasma confirm the effective removal of hemicellulose and lignin during the treatments and the production of cellulosic samples free of impurities. The removal of the peaks related to the functional groups of lignin and hemicellulose was in accordance with the results of the study by Harini et al. (2020) [30].

Band displacement  $cm^{-1}$   $2900$  is the higher wave number related to the stretching vibration of C-H groups, and a sharp decrease in the intensity of this band can confirm the presence of non-crystalline cellulose in the samples, which was in accordance with the results of the study of non-crystalline cellulose by Ciolako et al. (25) [25]. In the samples treated with cold plasma at a voltage of 20 kV and the sample treated before the alkaline and dye removal stage at a voltage of 18 kV in the region of  $cm^{-1}$  $2850$  new bands were created, which cannot be observed in the infrared spectrum of untreated and treated cellulose samples with an intensity of less than 18 kV. This band is related to CH-groups<sub>3</sub> is [26] and its observation after the application of 20 kV treatment and more intense treatment of 18 kV dielectric barrier plasma may be due to the

decomposition of cellulose and ultimately the production of -CH groups<sub>3</sub>be The decrease in the intensity of cellulose efficiency in these treatments (Table 2) can also be due to the decomposition of cellulose fibers.

### 3-3- Investigating the crystal structure

All samples showed peaks at  $16.49$ ,  $22.61$ , and  $34.67$  angles at  $2\theta$  angles, which indicate the type I cellulose crystal structure (Figure 2). The results show that the crystalline structure of cellulose was preserved in all samples and there was no change in the peak angles. Therefore, it can be said that chemical treatments and cold plasma treatment did not change the strength and cohesion of the primary cellulose crystal, however, the crystallinity index changed in the samples.

All samples showed higher crystallinity index and crystal size than raw walnut skin (Table 3), which is the result of removing non-crystalline parts (lignin and hemicellulose) from them and increasing the cellulose content of these samples [27]. These observations were consistent with the results of Fourier transform infrared spectroscopy.

After treating the samples with cold plasma, the crystallinity index and also the size of the crystals decreased slightly. This decrease after cold plasma treatment is due to the destruction of crystalline areas as a result of the radicals created during the treatment or decomposition due to the mechanism of scratching and breaking by plasma reactive species. As Gaoli et al. (2015) reported that hydroxyl radicals can effectively break hydrogen bonds and the crystal structure of cellulose [28]. In a study conducted by Vaneste et al. (2017) in investigating the effect of plasma treatment on lignocellulosic materials, they stated that ozone created by plasma in small amounts does not change the crystallinity index of cellulose, but with increasing treatment intensity and as a result removing lignin, the order The structure of lignocellulose is disturbed and causes the cellulose to become amorphous, and this crystallinity change can be reversed after the washing and drying process due to partial recrystallization [29].

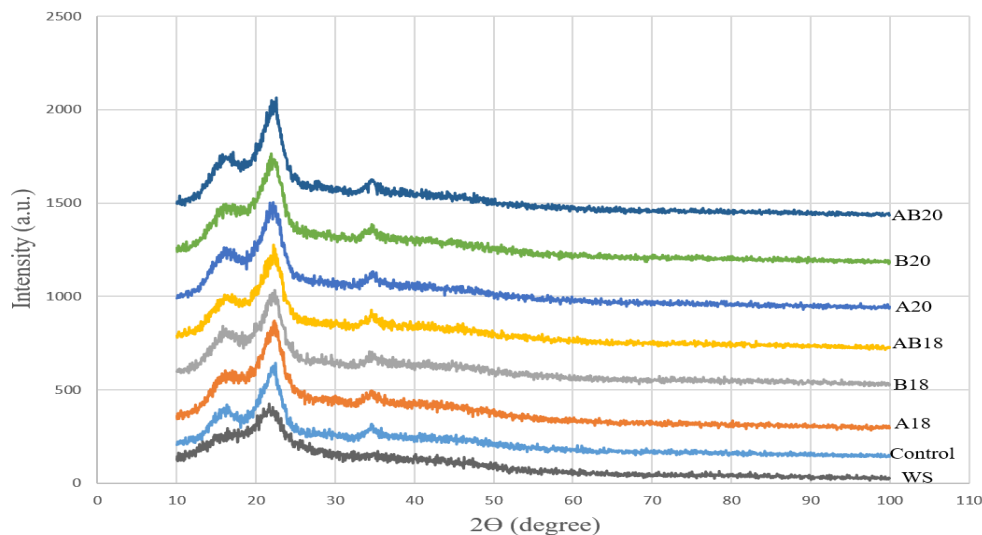


**Fig 2** X-ray diffractograms of Control, A18: Cellulose extracted by 18 kV plasma pretreatment before alkaline treatment, B18: Cellulose extracted by 18 kV plasma pretreatment before bleaching treatment, AB18: Cellulose extracted by 18 kV plasma pretreatment before alkaline and bleaching treatment, A20: Cellulose extracted by 20 kV plasma pretreatment before alkaline treatment, B20: Cellulose extracted by 20 kV plasma pretreatment before bleaching treatment, AB20: Cellulose extracted by 20 kV plasma pretreatment before alkaline and bleaching treatment, and WS: walnut shell.

**Table 3** Percentage of crystallization and crystal size of walnut shell and cellulose extracted by plasma treatment

| CrI (%) | L (°n) | b    | Sample  |
|---------|--------|------|---------|
| 34.9    | 1.14   | 7.36 | WS      |
| 59.8    | 2.63   | 3.20 | Control |
| 53.1    | 2.52   | 3.35 | A18     |
| 51.6    | 2.58   | 3.26 | B18     |
| 53.8    | 2.57   | 3.28 | AB18    |
| 54.1    | 2.51   | 3.35 | A20     |
| 53.1    | 2.59   | 3.25 | B20     |
| 55.7    | 2.58   | 3.26 | AB20    |

A18: Cellulose extracted by 18 kV plasma pretreatment before alkaline treatment, B18: Cellulose extracted by 18 kV plasma pretreatment before bleaching treatment, AB18: Cellulose extracted by 18 kV plasma pretreatment before alkaline and bleaching treatment, A20: Cellulose extracted by 20 kV plasma pretreatment before alkaline treatment, B20: Cellulose extracted by 20 kV plasma pretreatment before bleaching treatment, AB20: Cellulose extracted by 20 kV plasma pretreatment before alkaline and bleaching treatment, and WS: walnut shell.

### 3-4- Evaluation of thermal properties

In the comparison of thermogravimetric curves (Figure 3), three degradation stages were observed during the analysis of cellulose samples. Initial weight loss was observed for all samples at less than 150 degrees Celsius. This initial weight loss is related to the evaporation of moisture caused by the absorbed water in the samples [30]. This stage is a small peak on the left side of the differential thermogravimetric (DTG)

curve.<sup>12</sup>It is seen (Figure B3). Also, observing this peak in the DTG curves with the results of the presence of absorbed water in the region of  $\text{cm}^{-1}$  1641 FTIR curves are consistent. In the range of 30-100 degrees Celsius, which is related to the loss of moisture, the difference observed in the sample not treated with plasma and the treated sample is most likely related to free oxygen and weak hydrogen bonds in the fibers treated with plasma, compared to cellulose. Untreated, they react faster [20].

<sup>12</sup>. Differential thermogravimetric

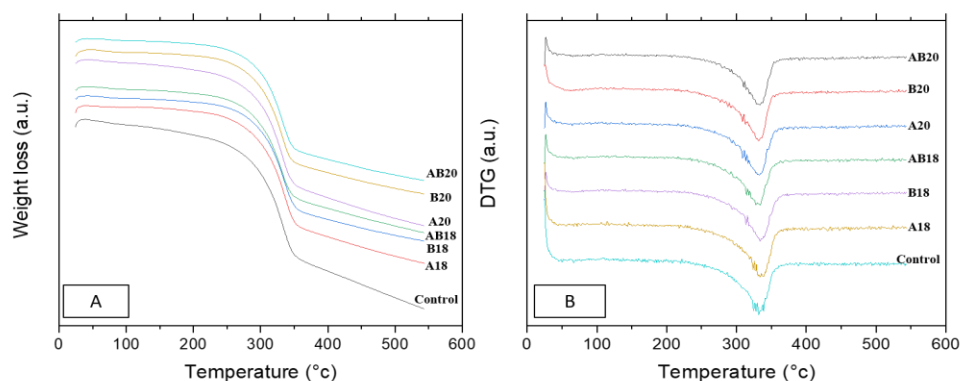


**Fig 3** (A) TGA and (B) DTG of Control, A18: Cellulose extracted by 18 kV plasma pretreatment before alkaline treatment, B18: Cellulose extracted by 18 kV plasma pretreatment before bleaching treatment, AB18: Cellulose extracted by 18 kV plasma pretreatment before alkaline and bleaching treatment, A20: Cellulose extracted by 20 kV plasma pretreatment before alkaline treatment, B20: Cellulose extracted by 20 kV plasma pretreatment before bleaching treatment, AB20: Cellulose extracted by 20 kV plasma pretreatment before alkaline and bleaching treatment, and WS: walnut shell

The main weight loss in the samples occurred in the temperature range of 250 to 370 degrees Celsius. In this stage, decarboxylation, depolymerization and destruction of cellulose units occur along with the formation of charcoal [31]. As can be seen, after the temperature of the start of destruction in this stage ( $T_{\text{onset}}$ ), the behavior of treated and untreated fibers was not significantly different until the final thermal decomposition, because the part under the influence of plasma, which includes free oxygen on the surface of the fibers, reacts faster than the cellulose structure, therefore, the thermal decomposition behavior is higher than the temperature  $T_{\text{onset}}$ . It remains unchanged [20].

The thermal degradation of the samples continued with a slight slope after 400 degrees Celsius and only a little thermal decomposition was observed after this temperature, which can be due to the higher carbonization of the polysaccharide chains produced by the breaking of C-H and C-C bonds and the breaking of the remaining coal into gaseous compounds with low molecular weight [32,30]. This stage progressed faster in the control cellulose sample than in other samples, which seems to be related to the remaining impurities such as hemicellulose and lignin in this sample compared to other samples [33]. The thermal behavior of hemicellulose, cellulose and lignin was investigated in studies and it was stated that the thermal degradation of hemicellulose, cellulose and lignin occurs in the temperature range of 210-

325, 310-400 and 160-900 degrees Celsius respectively [34]. As can be seen in the DTG curves (Figure B3), in the extracted samples, the degradation occurred in only one step from the temperature of 250 degrees Celsius to 370 degrees Celsius, and the maximum weight loss was observed at the temperature of 335 degrees Celsius. This temperature range is within the reported degradation temperature range. It is the destruction of cellulose that has been reported in other studies [35].

### 5-3- Investigating the microstructure of extracted cellulose

In order to better understand the effect of plasma treatment on the samples, the images obtained from the scanning electron microscope are shown in Figure 4 with a magnification of 10000. As can be seen in the figure, walnut bark shows a compact and lumpy structure, which indicates fibrous bundles together with non-fibrous compounds (hemicellulose and lignin) and waxes and other protective compounds in lignocellulosic materials that form a thick outer layer [27, 36].

Based on Figure 4, the cellulose fibers were well separated from the compressed structure of the walnut skin before being affected by cold plasma, and the surface of these cellulose fibers after removing the impurities shows a smooth structure without unevenness. After the plasma treatment, the samples first swelled, then holes were created



on the surface of the fibers and unevenness was created in some parts of the fiber, and the number of these holes increased by increasing the plasma voltage from 18 kV to 20 kV and increasing the number of times of plasma treatment. These chemical engravings are due to the collision of reactive species created in the plasma, which causes more hydrogen bonds to break in the cellulose fiber structure and destroy the cellulose structure, and also causes more impurities to be removed [37, 38]. The sample treated with 18 kV plasma before the alkaline treatment stage did not have severe changes compared to the control sample, and only some fiber swelling and

roughness can be seen on the surface of the fibers. According to Table 4, the average diameter of the fibers was affected by the applied treatment ( $p < 0.05$ ) and the average diameter of the fibers in the sample treated with 18 kV plasma before the alkaline stage increased compared to the control sample. This increase in diameter can be due to swelling of fibers. The changes in the sample treated under 18 kV plasma before the dyeing stage were more severe, so that the fibers became more swollen and some cracks and layering were observed on the surface of some fibers in the cellulose microfibers.

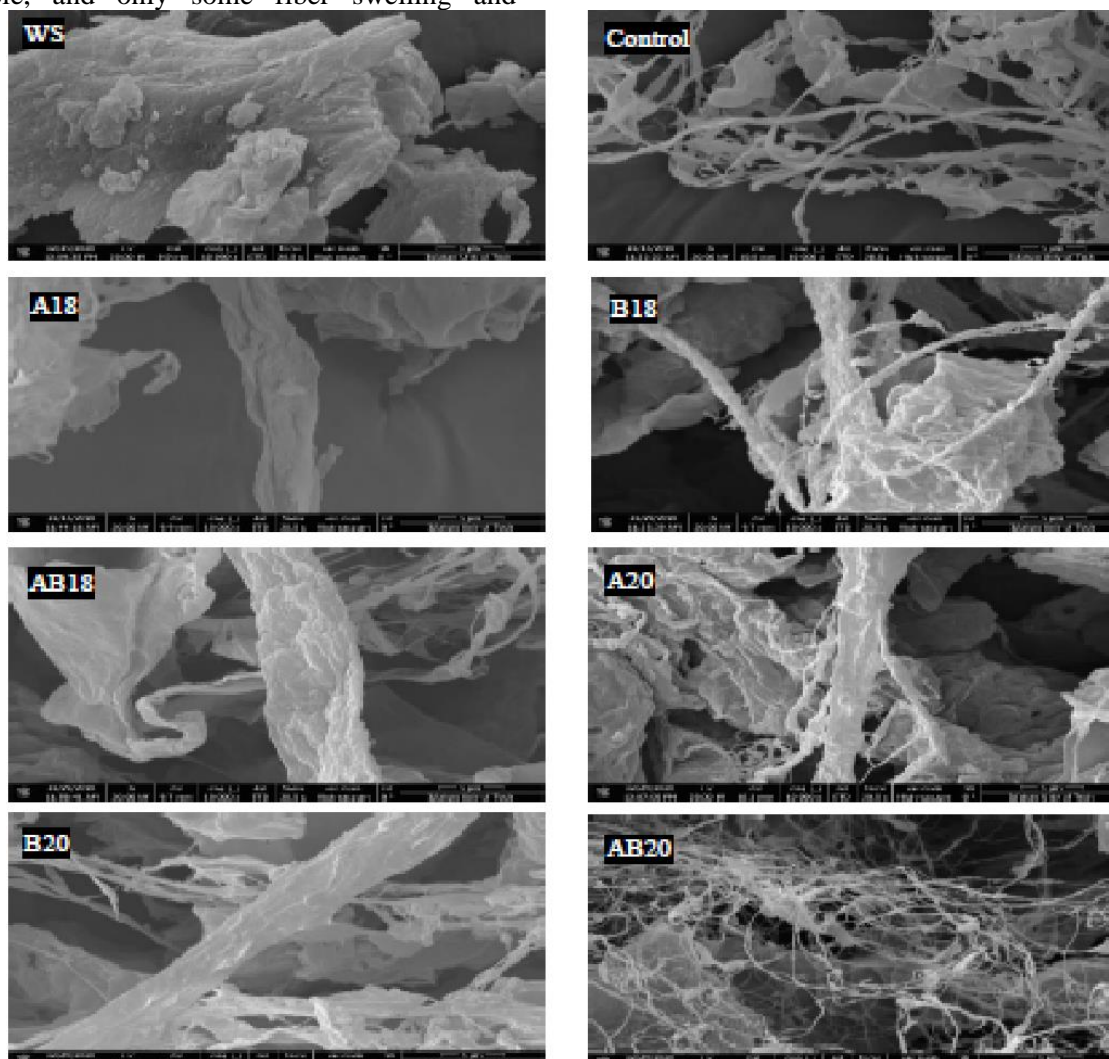


**Fig 4** FE-SEM images of Control, A18: Cellulose extracted by 18 kV plasma pretreatment before alkaline treatment, B18: Cellulose extracted by 18 kV plasma pretreatment before bleaching treatment, AB18: Cellulose extracted by 18 kV plasma pretreatment before alkaline and bleaching treatment, A20: Cellulose extracted by 20 kV plasma pretreatment before alkaline treatment, B20: Cellulose extracted by 20 kV plasma pretreatment before bleaching treatment, AB20: Cellulose extracted by 20 kV plasma pretreatment before alkaline and bleaching treatment, and WS: walnut shell.

This cracking and layering caused the average diameter of the fibers to decrease to  $0.52 \pm 0.11$  micrometers. Observing these changes in the sample treated before dyeing compared to the sample treated before alkaline treatment is probably due to the fact that in this sample the impurities were removed before plasma treatment and as a result the plasma reactive species had a more direct effect on cellulose fibers. After applying two stages of 18 kV plasma treatment during extraction, the degree of layering and separation of the strands from each other

increased and as shown in Figure 4, the level of unevenness on the fiber surface decreased, which could be due to the separation of strands and layers from the surface. fiber, and the average diameter of fibers showed a significant decrease to  $0.34 \pm 0.17$  micrometers (Table 4).

In the samples treated with 18 kV, carvings are observed in their surface layers, which appear as flaking at first, and with an increase in voltage and the number of times of exposure to plasma, the layers are almost completely removed due to more breakage in the bonds. be.

**Table 4** Average diameter of walnut shell fibers and cellulose extracted by plasma pretreatment

| The average diameter of fibers ( $\mu\text{m}$ ) | Sample  |
|--|---------|
| $3.38 \pm 1.15^A$                                | WS      |
| $0.81 \pm 0.10^{BC}$                             | Control |
| $0.98 \pm 0.25^B$                                | A18     |
| $0.52 \pm 0.11^{CD}$                             | B18     |
| $0.34 \pm 0.17^{OF}$                             | AB18    |
| $0.41 \pm 0.09^{OF}$                             | A20     |
| $0.26 \pm 0.10^{OF}$                             | B20     |
| $0.08 \pm 0.01^{AND}$                            | AB20    |

Various letters in each column show significant differences among mean values ( $p < 0.05$ ).

A18: Cellulose extracted by 18 kV plasma pretreatment before alkaline treatment, B18: Cellulose extracted by 18 kV plasma pretreatment before bleaching treatment, AB18: Cellulose extracted by 18 kV plasma pretreatment before alkaline and bleaching treatment, A20: Cellulose extracted by 20 kV plasma pretreatment before alkaline treatment, B20: Cellulose extracted by 20 kV plasma pretreatment before bleaching treatment, AB20: Cellulose extracted by 20 kV plasma pretreatment before alkaline and bleaching treatment, and WS: walnut shell.

In the sample treated under 20 kV plasma before the dyeing stage, holes are created on the surface of the fibers and the separation of fibers and the failure of the bonds are clear in this sample. In the sample that was subjected to two stages of 20 kV treatment, the separation of the connections and the failure of the connections caused the complete breakdown of the cellulose microfibrils into the nanocellulosic strands that make up them. As can be seen in Table 4, two stages of 20 kV treatment resulted in fibers with an average diameter of  $80 \pm 0.01$  nm. The results show that increasing the voltage from 18 to 20 kV has a great effect on the microstructure of the surface and the voltage change in a certain range is very sensitive. These results confirmed the results of Defaris et al. (2017) in investigating the effect of plasma on coconut fiber [38]. In the study of Bundelska et al. (2014) in the treatment of sugarcane bagasse fibers under the effect of microwave plasma in a period of 2 minutes, it was observed that the surface of the treated samples cracked significantly due to the effects of active species from the plasma and holes appeared on the surface. By increasing the treatment time to 5

minutes, layering and tearing of fibers were observed [39].

## 4 - Conclusion

In this study, the effect of non-thermal plasma pretreatment on the efficiency of cellulose extraction and the characteristics of cellulose extracted from walnut bark was investigated. Based on the obtained results, atmospheric cold plasma, as a process with partially ionized gas phase, creates a chemically rich environment that causes chemical and physical changes in the structure of lignocellulose. The results showed that the plasma treatment is able to break the connections and bonds in the lignocellulosic structures, and this facilitates the dyeing and delignin reactions, and therefore has the ability to increase the purity of cellulose. The change in the intensity of the bands related to FTIR along with the analysis of the chemical composition of cellulose showed that the use of cold plasma in combination with alkaline chemical treatments and dyeing not only effectively reduced the amount of hemicellulose and lignin impurities. Electron microscope images showed that due to

surface bombardment by reactive species resulting from plasma and surface wear mechanism, at lower voltage (18 kV) and less number of plasma treatments, swelling, scratches and unevenness were created on the surface of the fibers and with increasing voltage At 20 kV and increasing the number of times of plasma treatment, the amount of scratches and unevenness increased and ultimately led to more breakage of connections and cellulose fiber decomposition, reducing the extraction efficiency. Also, plasma treatment decreased the crystallinity of the samples. The results of this study showed that increasing the voltage from 18 to 20 kV has a great effect on the characteristics of extracted cellulose, so that by increasing the plasma voltage to 20 kV and applying it in both stages before alkaline treatment and before dyeing, nanofibers Cellulose with a diameter of 80 nm was obtained. Since a combination of chemical acid treatments with other mechanical treatments is used to prepare cellulose nanofibers, and in this study, cellulose nanofibers were obtained without using acidic chemicals and only by non-thermal plasma treatment, so it can be said that this process is a method It is effective and environmentally friendly in the preparation of cellulose nanofibers.

## 5- Resources

- [1] Trache, D., Hussin, M.H., Chuin, C.T.H., Sabar, S., Fazita, M.N., Taiwo, O.F., Hassan, T, and Haafiz, M.M, 2016, Microcrystalline cellulose: Isolation, characterization and biocomposites application—A review, *International Journal of Biological Macromolecules*, 93:789-804.
- [2] Merci, A., Urbano, A., Grossmann, M.V.E, Tischer, C.A., and Mali, S., 2015, Properties of microcrystalline cellulose extracted from soybean hulls by reactive extrusion, *Food Research International*, 73:38-43.
- [3] Okhamafe, A., Igboechi, A., Obaseki T, 1991, Celluloses extracted from groundnut shell and rice husk 1: preliminary physicochemical characterization, *Pharm World J*, 8(4):120-130.
- [4] Ting, S.S., 2019, Comparative Properties Analysis between Microcrystalline Cellulose and Cellulose Nanocrystals Extracted From Rice Straw, *Malaysian Journal of Microscopy*, 15(1):146-154.
- [5] Katakajwala, R, Mohan, S.V., 2020, Microcrystalline cellulose production from sugarcane bagasse: Sustainable process development and life cycle assessment, *Journal of Cleaner Production*, 249:119342.
- [6] Ren, H., Shen, J., Pei, J., Wang, Z., Peng, Z., Fu, S., and Zheng, Y., 2019, Characteristic microcrystalline cellulose extracted by combined acid and enzyme hydrolysis of sweet sorghum, *Cellulose*, 26(15):8367-8381.
- [7] Pérez, J., Muñoz-Dorado, J., De la Rubia, T., Martínez, J., 2002, Biodegradation and biological treatments of cellulose, hemicellulose, and lignin: an overview, *International Microbiology*, 5(2):53-63.
- [8] Nguyen, X.T., 2006, Process for preparing microcrystalline cellulose. US. Patent 7005514.
- [9] Junadi, N., Beg, M., Yunus, R.M., Ramli, R., Zianor Azrina, Z., Moshuiul Alam, A., 2019, Characterization of microcrystalline cellulose isolated through the mechanochemical method, *Indian Journal of Fibre & Textile Research (IJFTR)*, 44(4):442-449.
- [10] Stupińska, H., Iller, E., Zimek, Z., Wawro, D., Ciechańska, D., Kopania, E., et al, 2007, An environment-friendly method to prepare microcrystalline cellulose, *Fibres & Textiles in Eastern Europe*, 15:167-72.
- [11] Bárdos, L., Baránková, H., 2010, Cold atmospheric plasma: Sources, processes, and applications. *Thin Solid Films*, 518(23):6705-6713.
- [12] Pankaj, S., Wan, Z., Keener, K., 2018, Effects of cold plasma on food quality: A review, *Foods*, 7: 4.
- [13] Pankaj, S., Thomas, S., 2016, Cold plasma applications in food packaging, *Cold Plasma in Food and Agriculture: Elsevier*, 293-307.
- [14] Tendero, C., Tixier, C., Tristant, P., Desmaison, J., Leprince, P., 2006, Atmospheric pressure plasmas: A review, *Spectrochimica Acta Part B: Atomic Spectroscopy*, 61(1):2-30.
- [15] Souza-Corrêa, J., Oliveira, C., Nascimento, V., Wolf, L., Gómez, E., Rocha, G., et al, 2014, Atmospheric pressure plasma pretreatment of sugarcane bagasse: the influence of biomass particle size in the ozonation process, *Applied biochemistry, and biotechnology*, 172(3):1663-1672.
- [16] Shaghaleh, H., Xu, X., Liu, H., Wang, S., Hamoud, Y.A., Dong, F., et al, 2019, The effect of atmospheric pressure plasma pretreatment with various gases on the structural characteristics and chemical composition of wheat straw and applications to enzymatic hydrolysis, *Energy*, 176:195-210.
- [17] Hemmati, F., Jafari, S.M., Kashaninejad, M., Motlagh, M.B., 2018, Synthesis and

- characterization of cellulose nanocrystals derived from walnut shell agricultural residues, *International journal of biological macromolecules*, 120:1216-1224.
- [18] Kian, L.K., Jawaid, M., Ariffin, H., Alothman, O.Y., 2017, Isolation and characterization of microcrystalline cellulose from roselle fibers, *International journal of biological macromolecules*, 103:931-940.
- [19] Kumar, A., Negi, Y.S., Choudhary, V., Bhardwaj, N.K., 2014, Characterization of cellulose nanocrystals produced by acid-hydrolysis from sugarcane bagasse as agro-waste, *Journal of Materials Physics and Chemistry*, 2(1):1-8.
- [20] Macedo, M.J.P.d, 2018, Modification of kapok fibers by cold plasma surface treatment for the production of composites of recycled polyethylene. Ph.D. Dissertation, Universidade Federal do Rio Grande do Norte.
- [21] Moosavinejad, S.M., Madhoushi, M., Vakili, M., Rasouli, D., 2019, Evaluation of degradation in chemical compounds of wood in historical buildings using FT-IR and FT-Raman vibrational spectroscopy, *Maderas Ciencia y tecnología*, 21(3):381-92.
- [22] Bano, S., Negi, Y.S., 2017, Studies on cellulose nanocrystals isolated from groundnut shells, *Carbohydrate polymers*, 157:1041-1049.
- [23] Macedo, M.J., Silva, G.S., Feitor, M.C., Costa, T.H., Ito, E.N., Melo, J.D., 2020, Surface modification of kapok fibers by cold plasma surface treatment. *Journal of Materials Research and Technology*, 9: 2467-2476.
- [24] Shah, M.A., Khan, .M, Kumar, V., 2018, Biomass residue characterization for their potential application as biofuels, *Journal of Thermal Analysis and Calorimetry*, 134(3):2137-2145.
- [25] Ciolacu, D., Ciolacu, F., Popa, V.I., 2011, Amorphous cellulose—structure and characterization, *Cellulose chemistry and technology*, 45(1):13-2.
- [26] Țucureanu, V., Matei, A., Avram, A.M., 2016, FTIR spectroscopy for carbon family study, *Critical reviews in analytical chemistry*, 46(6):502-520.
- [27] Debiagi, F., Faria-Tischer, P.C., Mali, S., 2020, Nanofibrillated cellulose obtained from soybean hull using simple and eco-friendly processes based on reactive extrusion, *Cellulose*, 27(4):1975-1988.
- [28] Gao, L., Li, D., Gao, F., Liu, Z., Hou, Y., Chen, S., et al, 2015, Hydroxyl radical-aided thermal pretreatment of algal biomass for enhanced biodegradability, *Biotechnology for biofuels*, 8(1):1-11.
- [29] Vanneste, J., Ennaert, T., Vanhulsel, A., Sels, B., 2017, Unconventional pretreatment of lignocellulose with low-temperature plasma, *ChemSusChem*, 10(1):14-31.
- [30] Harini, K., Mohan, C.C., 2020, Isolation and characterization of micro and nanocrystalline cellulose fibers from the walnut shell, corncob, and sugarcane bagasse, *International Journal of Biological Macromolecules*, 163:1375-1383.
- [31] Trache, D., Donnot, A., Khimeche, K., Benelmir, R., Brosse, N., 2014, Physico-chemical properties and thermal stability of microcrystalline cellulose isolated from Alfa fibres. *Carbohydrate Polymers*, 104:223-30.
- [32] Kasiri, N., Fathi, M., 2018, Production of cellulose nanocrystals from pistachio shells and their application for stabilizing Pickering emulsions, *International journal of biological macromolecules*, 106:1023-1031.
- [33] Kian, L., Saba, N., Jawaid, M., Fouad, H., 2020, Characterization of microcrystalline cellulose extracted from olive fiber, *International journal of biological macromolecules*, 156:347-353.
- [34] Uzun, B., Yaman, E., 2015, Thermogravimetric pyrolysis of walnut shell an assessment of kinetic modeling. *International Conference on Industrial Waste and Waste Water Treatment Valorization*, held in Athens, Greece 21st–23rd May.
- [35] Kian, L.K., Saba, N., Jawaid, M., Fouad, H., 2020, Properties and characteristics of nanocrystalline cellulose isolated from olive fiber, *Carbohydrate Polymers*, 241: 116423
- [36] Abdullah, M., Nazir, M., Raza, M., Wahjoedi, B., Yussof, A., 2016, Autoclave and ultra-sonication treatments of oil palm empty fruit bunch fibers for cellulose extraction and its polypropylene composite properties, *Journal of cleaner production*, 126:686-697.
- [37] Kusano, Y., Madsen, B., Berglund, L., Oksman, K., 2019, Modification of cellulose nanofibre surfaces by He/NH<sub>3</sub> plasma at atmospheric pressure, *Cellulose*, 26(12):7185-7194.
- [38] de Farias, J.G.G., Cavalcante, R.C., Canabarro, B.R., Viana, H.M., Scholz, S., Simão, R.A., Surface lignin removal on coir fibers by plasma treatment for improved adhesion in thermoplastic starch composites, *Carbohydrate Polymers*, 165:429-436
- [39] Bundaleska, N., Tatarova, E., Dias, F., da Silva, M.L., Ferreira, C., Amorim, J., 2013, Air–water ‘tornado’-type microwave plasmas applied for sugarcane biomass treatment, *Journal of Physics D: Applied Physics*, 47(5):055201.



## بررسی ویژگی های سلولز استخراجی از پوست چوبی گردو با استفاده از پیش تیمار پلاسمای غیر حرارتی

انسیه سادات اناری<sup>۱</sup>، نفیسه سلطانیزاده<sup>۲\*</sup>

۱- کارشناس ارشد، گروه علوم و مهندسی صنایع غذایی، دانشکده کشاورزی، دانشگاه صنعتی اصفهان، اصفهان، ایران.

۲- دانشیار گروه علوم و مهندسی صنایع غذایی، دانشکده کشاورزی، دانشگاه صنعتی اصفهان، اصفهان، ایران.

| اطلاعات مقاله  | چکیده  |
|--|--|
| <p>تاریخ های مقاله :</p> <p>تاریخ دریافت: ۱۴۰۱/۰۴/۰۸</p> <p>تاریخ پذیرش: ۱۴۰۱/۱۲/۲۴</p> <p>کلمات کلیدی:</p> <p>پلاسمای سد دی الکتریک، سلولز، پوست گردو، ویژگی های ساختاری.</p> <p>DOI: 10.22034/FSCT.20.134.17</p> <p>DOR: 20.1001.1.20088787.1402.20.134.2.6</p> <p>* مسئول مکاتبات: <a href="mailto:soltanizadeh@iut.ac.ir">soltanizadeh@iut.ac.ir</a></p> | <p>مطالعه حاضر، با هدف استخراج سلولز از پوست چوبی گردو با استفاده از پیش تیمار پلاسمای سد دی الکتریک و بررسی ویژگی های آن انجام شد. بدین منظور پوست چوبی گردو در سه مرحله در معرض پلاسمای سد دی الکتریک در دو ولتاژ ۱۸ و ۲۰ کیلوولت به مدت ۱۰ دقیقه قرار گرفت. در مرحله اول، این فرآیند قبل از تیمار قلیایی با سدیم هیدروکسید، در مرحله دوم قبل از تیمار رنگبری با سدیم کلریت و در نهایت این پیش تیمار هم قبل از تیمار قلیایی و هم قبل از رنگبری اعمال شد. آزمون های بازده استخراج، طیف سنج مادون قرمز تبدیل فوریه (FTIR)، ساختار بلوری (XRD)، ویژگی های حرارتی (TGA)، ریزساختار نمونه ها (FE-SEM) و بررسی قطر الیاف انجام شد. بر اساس نتایج، بازده استخراج سلولز تحت تاثیر ولتاژ اعمال شده قرار گرفت (<math>p &lt; 0/05</math>) و به دلیل تاثیر پلاسمای در شکست پیوندها بازده کاهش یافت. طیف سنج مادون قرمز حذف پیک های مربوط به ناخالصی ها و خلوص فیبرهای سلولز استخراجی را تایید کرد. نتایج، عدم تغییر ساختار بلوری سلولز را نشان داد اما کاهش شاخص بلورینگی رخ داد. اثر پلاسمای در وزن سنج حرارتی نمونه ها در دماهای زیر ۱۰۰ درجه سلسیوس مشاهده شد و بعد از دمای شروع تخریب رفتار فیبرهای تیمار شده و نشده تا تجزیه حرارتی نهایی تفاوت قابل ملاحظه ای نداشت. در تصاویر میکروسکوپ الکترونی نمونه های تیمار شده با پلاسمای در ابتدا تورم و ناهمواری در سطح مشاهده شد که در ولتاژهای بالاتر سبب شکست بیشتر اتصالات شده و نانوفیبرهایی با قطر ۸۰ نانومتر به وجود آمدند. به طور کلی نتایج نشان داد اعمال پلاسمای با ولتاژ ۲۰ کیلوولت در هر دو مرحله قبل از تیمار قلیایی و قبل از رنگبری، تیمار مناسب تری برای استخراج سلولز و تولید نانوالیاف سلولزی است.</p> |